AGU100 ADVANCING EARTH AND SPACE SCIENCE

Geophysical Research Letters

RESEARCH LETTER
10.1029/2018GL077955

Key Points:
- A model ensemble suggests that dynamical variability dominates ozone recovery trends in the tropical and midlatitude lower stratosphere
- Upper stratospheric ozone is expected to display the largest recovery at high latitudes in both hemispheres in autumn/winter seasons
- Solar proton events need to be taken into account when evaluating upper stratospheric ozone recovery

Supporting Information:
- Supporting Information S1

Correspondence to:
K. A. Stone,
stonek@mit.edu

Citation:
Stone, K. A., Solomon, S., & Kinnison, D. E. (2018). On the identification of ozone recovery. *Geophysical Research Letters*, *45*. https://doi.org/10.1029/2018GL077955

Received 15 MAR 2018
Accepted 6 MAY 2018
Accepted article online 14 MAY 2018

On the Identification of Ozone Recovery

Kane A. Stone[1], Susan Solomon[1], and Douglas E. Kinnison[2]

[1]Department of Earth, Atmospheric, and Planetary Science, Massachusetts Institute of Technology, Cambridge, MA, USA, [2]Atmospheric Chemistry Observations and Modeling Laboratory, National Center for Atmospheric Research, Boulder, CO, USA

Abstract As ozone depleting substances decline, stratospheric ozone is displaying signs of healing in the Antarctic lower stratosphere. Here we focus on higher altitudes and the global stratosphere. Two key processes that can influence ozone recovery are evaluated: dynamical variability and solar proton events (SPEs). A nine-member ensemble of free-running simulations indicates that dynamical variability dominates the relatively small ozone recovery signal over 1998–2016 in the subpolar lower stratosphere, particularly near the tropical tropopause. The absence of observed recovery there to date is therefore not unexpected. For the upper stratosphere, high latitudes (50–80°N/S) during autumn and winter show the largest recovery. Large halogen-induced odd oxygen loss there provides a fingerprint of seasonal sensitivity to chlorine trends. However, we show that SPEs also have a profound effect on ozone trends within this region since 2000. Thus, accounting for SPEs is important for detection of recovery in the upper stratosphere.

Plain Language Summary With the continuing decline in ozone depleting substances, upper-atmospheric ozone is displaying signs of healing in the Antarctic region. Using a state-of-the-art model that simulates the Earth system, the nature of future ozone recovery outside of the Antarctic region is investigated to identify potential fingerprints for observing future ozone recovery. The model results show that ozone recovery near 40 km is expected to be largest near the poles in both hemispheres during winter and spring, while there is still large variability in the tropical region. However, energetic protons from solar events also have an effect on ozone in these regions through well-known chemical mechanisms. Therefore, taking these effects into account will be important for detecting this ozone recovery in observations.

1. Introduction

In the late 20th century, stratospheric ozone began to decline due to anthropogenic emissions of ozone depleting substances (ODSs), particularly chlorofluorocarbons. This caused concern since stratospheric ozone shields the Earth's surface from DNA damaging radiation. However, now, with the expected continued decline in equivalent effective stratospheric chlorine (EESC) due to the Montreal Protocol, ozone ceased its decline and began its slow healing process (also referred to here as recovery) near the turn of the 21st century. Healing is expected to become increasingly detectable in observations and has been a prime focus of ozone research. Multiple studies have shown signs of Antarctic ozone recovery (Kuttippurath & Nair, 2017; Solomon et al., 2016; Strahan and Douglass, 2018). In this study, the detection of ozone recovery outside the ozone hole region is investigated on a monthly and latitudinal basis from a model perspective.

In addition to changes in ODS and greenhouse gas-induced effects on climate and their impact on stratospheric ozone (Jonsson et al., 2004; Li et al., 2009), other drivers that are known to affect ozone on annual or decadal time scales include the following: the quasi-biennial oscillation (Baldwin et al., 2001); the solar cycle (e.g., Merkel et al., 2011; Steinbrecht et al., 2004); tropospheric influences, such as El Niño–Southern Oscillation (ENSO; Camp et al., 2003; Xie et al., 2014); changes in planetary wave forcings, typically expressed as changes in heat flux (e.g., Shaw & Perlwitz, 2014); volcanic aerosols (Portmann et al., 1996; Solomon et al., 1998); and solar proton events (SPEs) (Jackman et al., 1999; Jackman et al., 2008); or a combination of variables, such as the QBO and solar cycle (Camp & Tung, 2007). Studies have indicated that short-term variability from the drivers listed above may be masking recovery in the global averaged total column ozone and upper stratospheric ozone (Chipperfield et al., 2017; Harris et al., 2015; Steinbrecht et al., 2017; Tummon et al., 2015). This in turn may link to reports of a recent decline in tropical lower stratospheric ozone (Ball et al., 2018), although data set uncertainties and quality have also been highlighted, especially when merging different data sets (Steinbrecht et al., 2017; Tummon et al., 2015). Furthermore, there are large uncertainties in tropospheric ozone trends (which accounts for around 10% of the ozone column), which can thus influence total

ozone trend detection (Ball et al., 2018). While the real world represents only one realization, the range of expected dynamical variability can be examined using an ensemble of multiple realizations of a chemistry-climate model. An ensemble analysis is presented here to illustrate where dynamical variability may be expected to be large compared to chemical recovery.

SPEs produce ion pairs that alter the odd nitrogen (NO_x) and odd hydrogen (HO_x) cycles in the upper stratosphere and mesosphere, thus causing excess ozone depletion in the polar cap region. The SPE-induced ozone loss from HO_x chemistry lasts only a few hours but NO_x can cause stratospheric ozone loss for months after the SPE. These events occur at higher latitudes and have their largest effects during the fall and winter months (Jackman et al., 1999; Jackman et al., 2008; Jackman et al., 2009; Solomon & Crutzen, 1981). The SPE events during July 2000 and October 2003 are some of the largest on record and are near the EESC turn around time (Jackman et al., 2008). Multiple linear regression is used here to account for the short-term drivers in ozone variability including SPEs (see the supporting information for methods).

2. Model Description

The Community Earth System Model, version 1 (CESM1) is a fully coupled climate model that incorporates atmosphere, ocean, land, and sea ice modules (Marsh et al., 2013). The atmosphere module is the Whole Atmosphere Community Climate Model, version 4 (WACCM4) that has a horizontal resolution of 1.9° latitude by 2.5° longitude and up to 88 vertical levels with a high top at 5.1×10^6 hPa (~140 km). The chemical scheme used is the Model of OZone And Related Tracers (Kinnison et al., 2007) and includes 183 different species, 341 gas phase reactions, 114 photolytic processes, and 17 heterogeneous reactions on multiple aerosol types. This chemical scheme has been shown to accurately simulate Antarctic ozone depletion and levels of chlorine reservoir species (Solomon et al., 2015, 2016).

Using this model, two simulation setups are used, a specified dynamics version of the model, and a fully coupled ensemble. In the specified dynamics version, the fields of temperature, zonal wind, meridional wind, and surface pressure are nudged to Modern-Era Retrospective analysis for Research and Applications (MERRA) at 88 vertical levels. We use a Chemistry-only simulation (Chem-only), where the dynamical conditions are fixed to 1999 levels over 1999–2014, and a simulation with time-evolving specified MERRA dynamics over 1999–2014 as well as sulfate area densities from Neely and Schmidt (2016) (Chem-dyn-vol); see Mills et al. (2016) and Solomon et al. (2016) for further details. The fully coupled ensemble uses a free running atmosphere-ocean chemistry climate general circulation model whose nine members are run over the 1995–2024 period, allowing examination of both trends to date and to what extent additional years of observation should be expected to display more robust trends. These simulations have a repeated cyclic 28-month QBO, no solar cycle or SPEs, and 66 vertical levels. Initialization of the ensembles follows the approach in Solomon et al. (2017).

3. Results

Ozone trends over the period of 2000–2014 are calculated for the Chem-only simulation and over both 1998–2016 and 1998–2024 for the ensemble simulations. The linear trend was extracted using multiple linear regression. For the Chem-only simulation, the regression model uses 10.7 cm solar flux to account for solar brightness changes, and an NO_2 concentration regression function extracted from the Chem-only simulation. The NO_2 predictor acts as a proxy for the SPE events (the justification for which is shown below in Figures 3 and S1 and S2, where large NO_2 concentrations caused by SPEs coincide with large negative ozone anomalies in the model runs and in the equivalent latitude filled Stratospheric Water and OzOne Satellite Homogenized [SWOOSH] data set, v2.6; where available; Davis et al., 2016). The NO_2 proxy was preprocessed by removing the mean over the solar minimum period of 2008–2011. However, the solar cycle or linear trends were not removed. Therefore, considering that the sign of the NO_2 linear trends are opposite to that of ozone, this proxy will act to slightly over fit the ozone linear trends. We also note that a comprehensive set of significant SPEs, as considered in Jackman et al. (2009), were included in the regression, and their impact on NO_2 over both polar regions at 2 hPa is shown in Figure S2. The ensemble simulations were produced without a solar cycle or SPEs since these can be dealt with via regression as the Chem-only simulation shows. The regression functions used for the ensemble simulations include QBO_{10}, QBO_{30}, ENSO, and 100 hPa heat flux over 40–80°N/S. The QBO subscripts designate the hPa pressure level of the zonal wind field averaged between

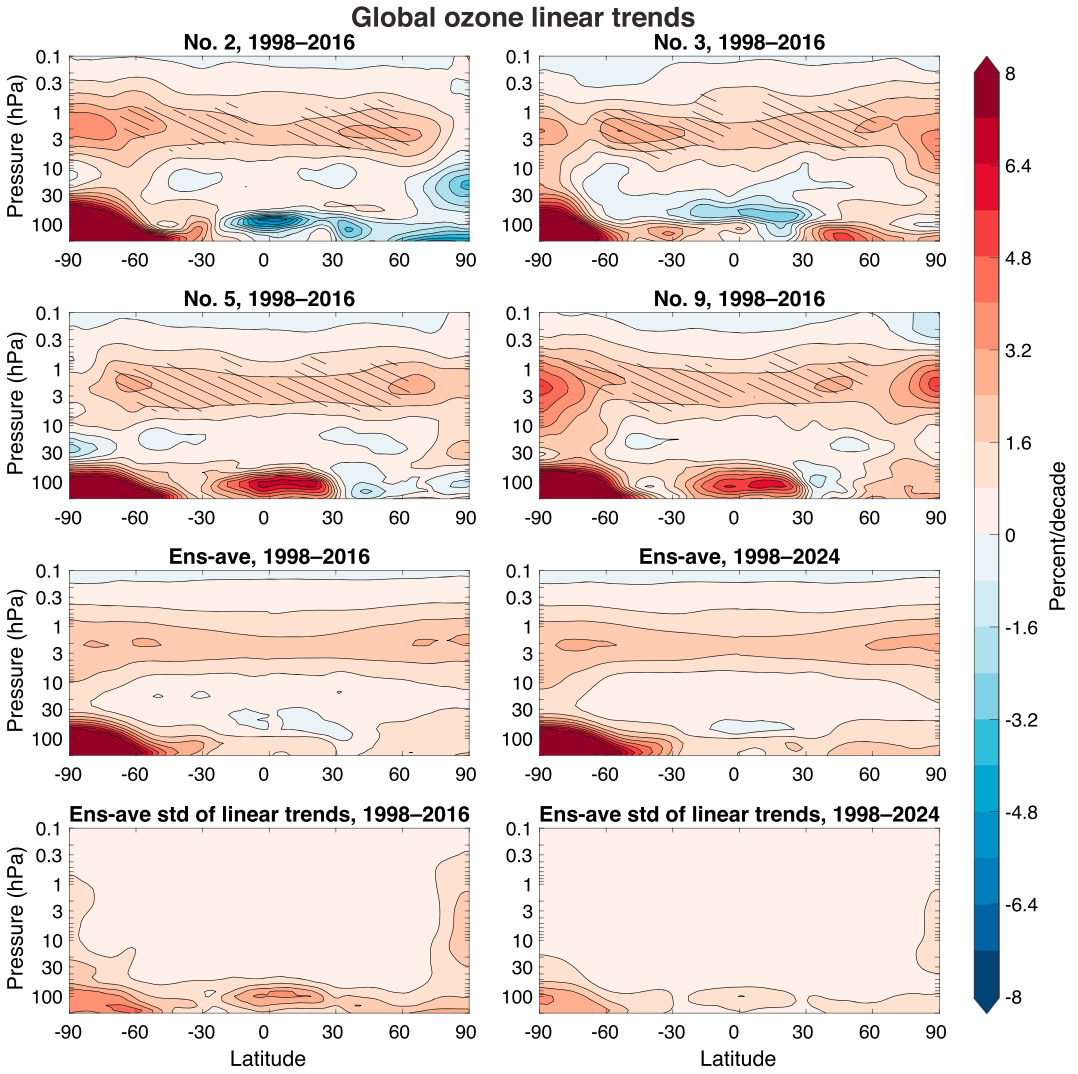

Figure 1. Zonal mean linear trends over 1998–2016 for four individual members that showed the largest variation in the lower stratosphere (top four panels). Stippling shows trend magnitude greater than 2σ uncertainties. Zonal mean linear trends for Ens-ave over 1998–2016 and 1998–2024 and their associated standard deviations are shown to highlight reduced trend variability when the length of the time series is increased (bottom four panels).

−5°S and 5°N. Uncertainties on the trend are shown at the 2σ level following (Reinsel et al., 2002; Steinbrecht et al., 2017). Uncertainties are not shown for the ensemble average or Chem-only trends as the nine-member average and reduced variability in the Chem-only simulation return the trend greater than the 2σ level virtually everywhere in the upper stratosphere. (see the supporting information for more detailed methods). We also note that the distribution of the residuals after regression follows a normal distribution about zero (see Figure S7).

3.1. Ozone Variability in a Nine-Member Ensemble

Figure 1 presents linear trends calculated from multiple linear regression analysis of ensemble runs. The figure shows the ensemble mean trends for 1998–2016 and 1998–2024, along with four individual realizations for 1998–2016 to illustrate positive and negative extremes of trends in the lower stratosphere. The trend standard deviations about the nine-member means for 1998–2016 and 1998–2024 are also shown. Trends for all nine members are also shown individually for these periods in Figures S3 and S4, respectively. Figure S5 also shows trends for individual members using slightly different start and end dates around 1998–2016. Results outside the tropical lower stratosphere are not very sensitive to a few years variation around this time.

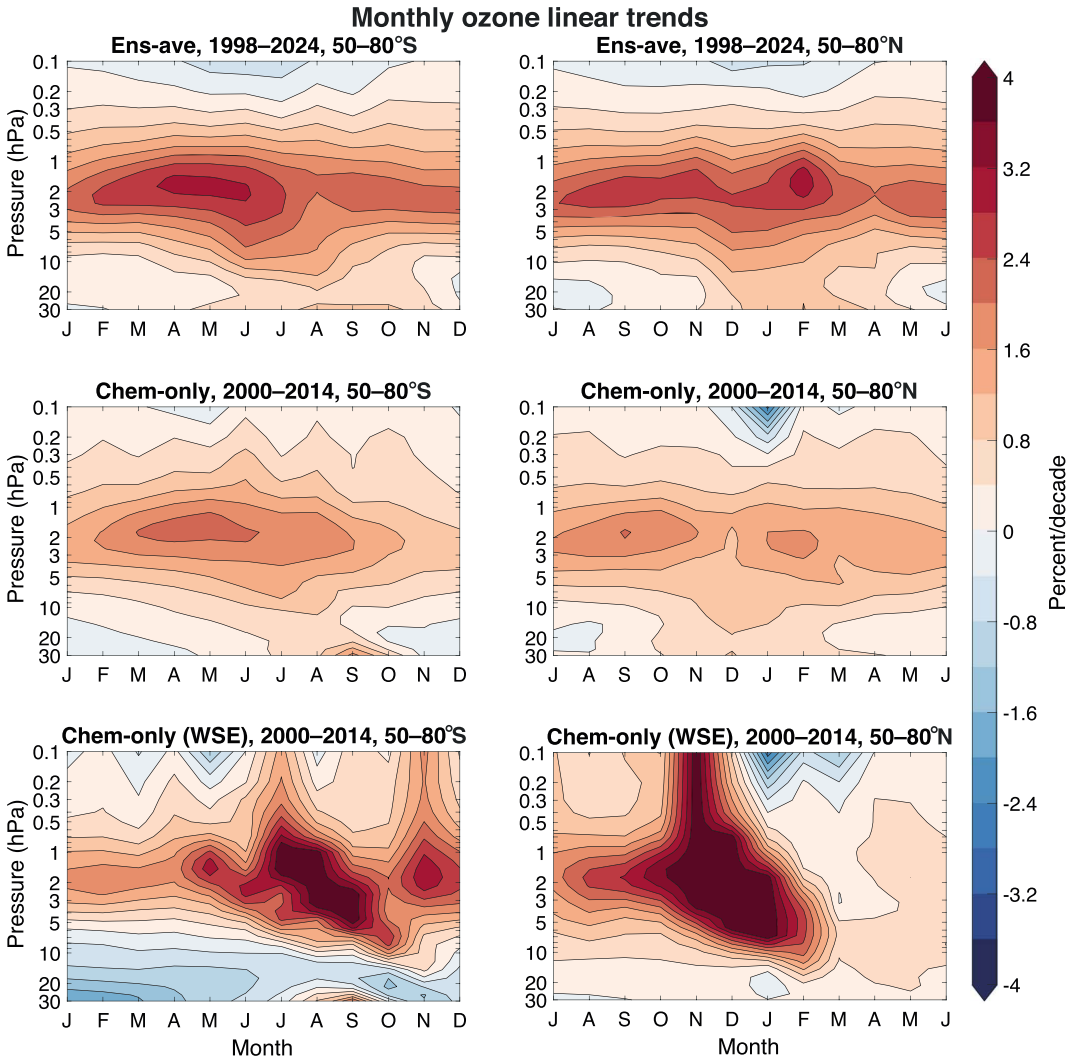

Figure 2. Pressure-month linear trends between 50 and 80°S/N. (top) The Ens-ave trends over 1998–2024, (middle) the Chem-only trends with solar and NO_2 regression functions over 2000–2014, and (bottom) the Chem-only linear trends without solar and NO_2 regression functions (i.e., with solar effects (WSE)) over 2000–2014.

The ensemble members display that trends in the lower stratosphere region outside the Antarctic are characterized by large variability for 1998–2016, ranging from values as large as about +6% per decade to −6% per decade in the tropics. The latter value is comparable to the negative trends in tropical observations presented in Ball et al. (2018). We find that these trends are not very sensitive to the regression, as was also noted by Ball et al. (2018); see Figure S6 for a comparison to simple linear trends for 1998–2024 with no multiple linear regression. In addition, in the tropical lower stratosphere and polar upper stratosphere, the model shows similar, although slightly elevated, variability in ozone percent anomalies compared to SWOOSH (see Figure S8). In summary, the figure suggests that dynamical variations currently dominate ozone trends in the model since the onset of ODS decline in the lower subpolar stratosphere, particularly in the tropical region highlighted in Ball et al. (2018). Note, however, that Figure 1 also shows that in the absence of unusual geophysical events (such as major volcanic eruptions), longer records over the next seven years or so should allow recovery to emerge more clearly in midlatitudes and the Arctic, and more representative trends to be observed in the tropics.

3.2. Identifying Ozone Recovery in the Upper Stratosphere, Including SPEs

All ensemble members display positive trends in the upper stratosphere, indicating recovery. To investigate the seasonality of chemical ozone recovery at high latitudes, Figure 2 shows monthly trends averaged

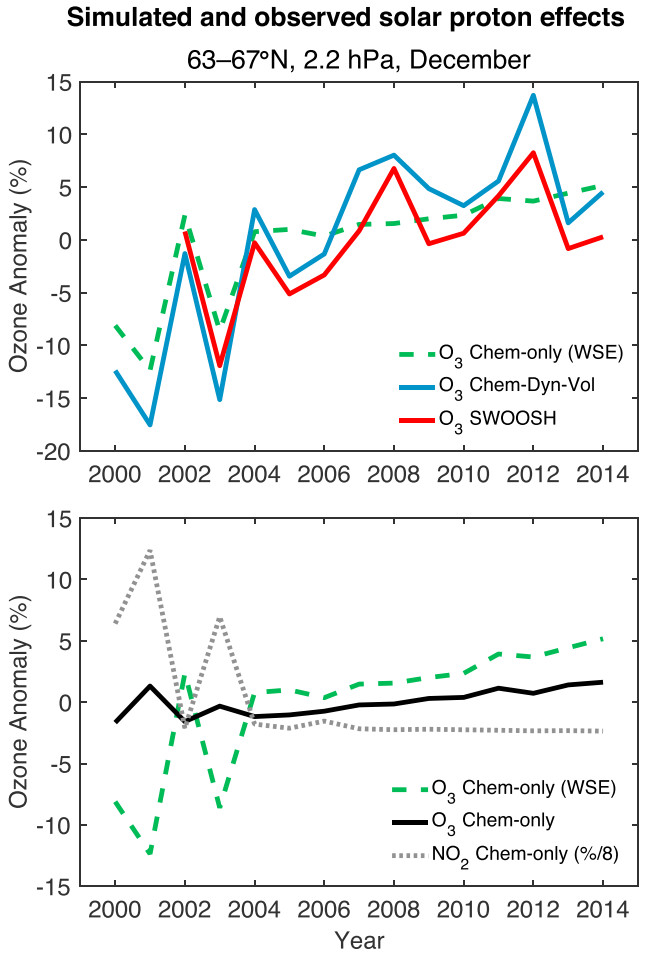

Figure 3. Time series of ozone anomalies in Chem-only, Chem-dyn-vol, SWOOSH for 63–67°N in December, which is a region that SPEs are seen to have large influences on ozone concentrations (top panel). To highlight how the regression removes the SPE influence, the Chem-only simulation with solar effects (WSE), the Chem-only simulation with solar effects removed via regression, and the NO_2 SPE proxy are shown (bottom).

between 50 and 80°S and 50 and 80°N. For the Chem-only simulation, the monthly trends are shown for two applications of the regression function, one using only a linear regression function (and therefore with solar effects [WSE] included in the time series) designated Chem-only (WSE), and the other using linear, solar, and NO_2 regression functions, and therefore WSE taken into account. Figure 1 shows that the large trends extend to 90°N. However, the limit of 80°N was chosen as 80–90°N also shows large variation in the trends between ensemble members, as shown in the standard deviations of linear trends in Figure 1. In the ensemble average, the largest trends are occurring mainly in the autumn and winter seasons in both hemispheres. The Chem-only simulation shows extremely similar results, and this seasonal cycle provides a fingerprint for recovery. The structure and timing of the largest ozone recovery trends mimic that of the ensemble average. This autumn/winter time period coincides with wintertime descending air, which has low concentrations of CH_4. This in turn leads to decreased concentrations of HCl and therefore allows for increased Cl and ClO and more ozone loss. In the time period of decreasing EESC trends (circa 1998 to present), it can be expected that the seasons and latitudes that are most strongly controlled by halogen chemistry will exhibit the largest ozone recovery trends (see the next section for further details).

In the Chem-only simulation (WSE, bottom panels), the linear regression does not yield similar structure as in the panels above. This is because the four largest SPEs, with ion pair production rates greater than $1{,}500 \cdot cm^{-3} \cdot s^{-1}$, occurred during July 2000, November 2000, November 2001, and October 2003 (see Jackman et al., 2009, and Figure S2). Since SPEs destroy ozone, the timing of the largest SPEs near the start of the time series acts to increase the ozone trends over 2000–2014. By removing these SPE effects, the results from the ensemble average can be reproduced (as seen in the Chem-only regression that includes solar and SPE regression functions in Figure 2).

Figure 3 further illustrates that the ozone changes due to SPEs in this region are substantial as compared to dynamical variability. The figure compares ozone anomalies for Chem-only, Chem-dyn-vol, and SWOOSH to the NO_2 SPE proxy for illustrative latitudes and pressure levels that are captured by both SWOOSH and WACCM simulations. Between 63 and 67°N, there are three large positive NO_2 anomalies during December 2000, 2001, and 2002 at 2.2 hPa associated with large ozone decreases in the model (and consistent with early studies by Seppälä et al., 2004). SWOOSH observations capture the 2002 event (but are not available for the earlier dates). The agreement between the Chem-dyn-vol and SWOOSH anomalies indicates that the impacts of SPEs are indeed captured by satellite observations to some extent and therefore can have a profound effect on trends, as can be seen by comparing the Chem-only linear trends that do and do not include solar predictors in Figure 2.

It is important to note that the effects of SPEs are occurring in the same latitudes and over the same seasonal time period as the largest ozone trends. Here we have shown that it is essential to account for these effects to identify the large autumn/winter high-latitude ozone recovery trends in the upper stratosphere.

3.3. Chemistry of High-Latitude Gas Phase Ozone Recovery

Upper stratospheric chemical ozone recovery has long been expected to maximize between about 3 and 1 hPa at higher latitudes due to the changing fraction of odd oxygen (O_x) loss by halogen chemistry (ClO_x + BrO_x; Newchurch et al., 2003), hereafter referred to as total O_x/ClO_x loss. Here we investigate this chemistry in further details. The main proposed mechanism for the large autumn/winter high-latitude gas phase recovery compared to other months and latitudes is the onset of wintertime descending air into the

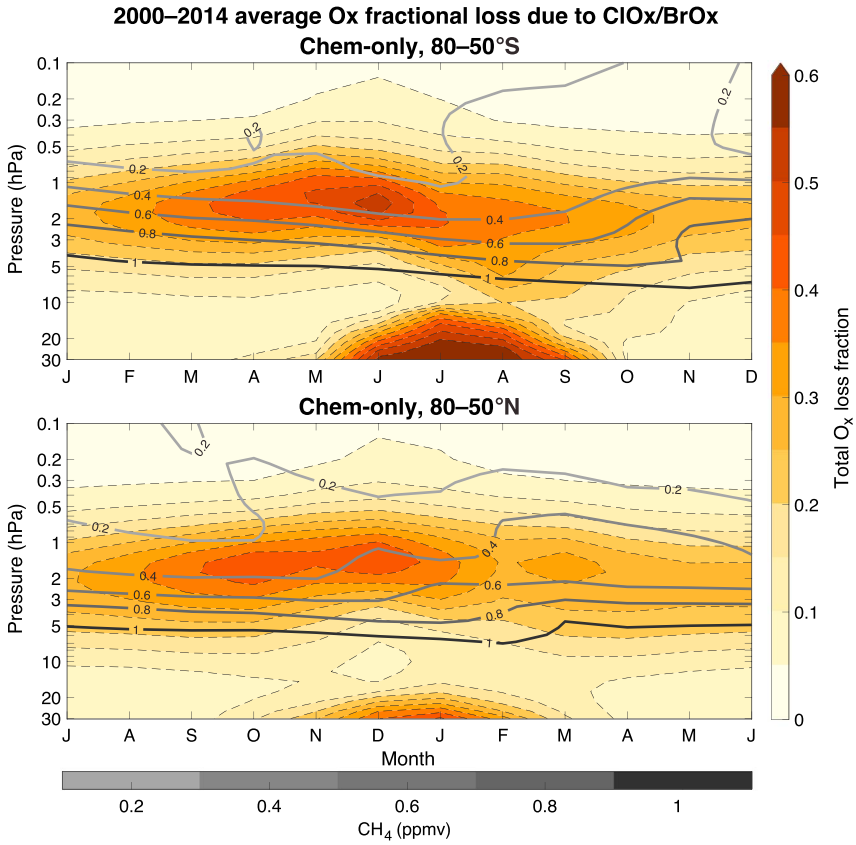

Figure 4. Month-pressure total O_x/ClO_x loss fraction for 50–80°S/N averaged over 2000–2014 (filled contours). To visualize the wintertime descending CH_4 and its impact on halogen chemistry, CH_4 concentrations are over plotted as line contours.

region of gas phase ozone chemistry (Solomon & Garcia, 1984). This descending air has lower CH_4 concentrations, which is important for the partitioning of Cl and ClO, with less chemically active chlorine converted into HCl (Solomon et al., 1985). This increases the total O_x/ClO_x loss, and as mentioned previously, means that the recent decreasing trend in EESC should present the largest ozone recovery trends in the regions and time periods where the total O_x/ClO_x loss is largest. To investigate this, Figure 4 shows the Chem-only simulated total O_x/ClO_x loss averaged over 2000–2014 for 50–80°S and 50–80°N. Line contours of CH_4 are plotted over the fraction of total O_x loss.

It is clearly seen that the largest total O_x/ClO_x loss is occurring in the autumn/winter seasons in both hemispheres. This agrees very well with the seasonal timing of largest subpolar chemistry-induced ozone recovery. Looking at the pressure levels between 3 and 1 hPa in the Southern Hemisphere, CH_4 concentrations are decreasing throughout the late summer, autumn, and winter seasons, with a minimum occurring in winter. At pressure levels above this, the minimum in CH_4 is occurring earlier in winter, and at lower levels, the minimum is occurring in late winter to early spring. The peak in total O_x/ClO_x loss at pressures between 3 and 1 hPa, of up to 0.55, is occurring in June, but with high fractions of up to 0.40 occurring from February through to August. The Northern Hemisphere shows similar results compared to the Southern Hemisphere, with large total O_x/ClO_x loss due to halogens occurring in the autumn and winter seasons. However, the values are slightly less, not exceeding 0.45 between 3 and 1 hPa, and not extending into the early spring season, as seen in the Southern Hemisphere. This coincides with the earlier increase of CH_4 at these pressure levels during December (early winter) compared to August (early spring) in the Southern Hemisphere.

The small differences in the hemispherical seasonal timing of CH_4 descent and the related changes in the total O_x/ClO_x loss agree well with the differences in the seasonal timing of largest ozone recovery that is

seen in the Chem-only simulation. This further solidifies that in the presence of decreasing chlorine, the seasonal modulation of total O_x/ClO_x loss is the main driver of the large seasonal ozone recovery trends in Chem-only, providing a useful fingerprint for recovery if SPE effects are accounted for as shown above.

4. Conclusions

With the onset of EESC decline in the late 1990s, the detection of ozone recovery has become an important focus in the atmospheric science community. Here we focus on (i) dynamical variability, particularly in the tropical lower stratosphere, and (ii) upper stratospheric ozone recovery trends in a full coupled chemistry climate model using two different setups, a nine-member ensemble using a free running setup over 1998–2016 and 1998–2024, and a chemistry only setup that has repeating 1999 specified dynamics over 2000–2014 (Chem-only). Linear trends were calculated using a multiple linear regression model with 10.7 cm solar flux and NO_2 (a proxy for SPEs) predictors for the Chem-only simulation, and with QBO, ENSO, and 100 hPa heat flux predictors for the ensemble simulations.

In the lower stratosphere outside the Antarctic, the individual ensemble members display large variations in ozone trends about zero since about the year 1998, impeding the identification of robust recovery (or depletion) trends. Particularly in the tropical lower stratosphere, our model suggests that dynamic variability could yield ozone trends since 1998 as large as +6% or −6% per decade, comparable to the values found in one recent study (Ball et al., 2018). Our simulations also show how seven additional years of observation should allow recovery to emerge more clearly in the subpolar lower stratosphere in midlatitudes, and a more representative small trend to be obtained in the tropics.

The largest upper stratospheric modeled trends are occurring at high latitudes in both hemispheres. By picking out the high-latitude regions of 50–80°S/N that show the largest global zonal average trends (with lower variability between ensemble members), we identified a seasonal fingerprint of recovery, with trends maximizing in the autumn/winter seasons in both hemispheres. This seasonal fingerprint arises due to descending autumn/winter air with low CH_4 concentrations (thus less HCl), and therefore allowing halogen chemistry to dominate odd oxygen loss. With recent decreasing chlorine levels, this corresponds to the regions and seasons of largest ozone recovery. However, this seasonal time period also marks the time period when SPEs have the largest effect on ozone depletion due to descending newly formed NO_2 (Jackman et al., 1999). These events are known to affect ozone primarily at high latitudes. Strong SPEs occurred early on in the 2000s, near the time of expected onset of ozone recovery, and it is shown here that these can have a profound effect on the value of linear ozone trends within both model and observational data over the ozone recovery period to date. Regression analyses including modeled (or observed) NO_2 are one way to account for these effects and better identify this distinctive recovery signature.

Acknowledgments

K. S. and S. S. were partially supported by NSF atmospheric chemistry division grant 1539972. D. K. was partially supported by the NASA LWS grant NNX14AH54G. The National Center for Atmospheric Research (NCAR) is sponsored by the U.S. National Science Foundation. WACCM is a component of the Community Earth System Model (CESM), which is supported by the National Science Foundation (NSF) and the Office of Science of the U.S. Department of Energy. Computing resources were provided by NCAR's Climate Simulation Laboratory, sponsored by NSF and other agencies. This research was enabled by the computational and storage resources of NCAR's Computational and Information System Laboratory (CISL). We thank NASA Goddard Space Flight Center for the MERRA data (accessed freely online at http://disc.sci.gsfc.nasa.gov/). We thank Sean Davis and Karen Rosenlof, from the National Oceanic and Atmospheric Administration, Chemical Sciences Division, for access to the SWOOSH ozone data set. Model results shown in this paper are available on request to Doug Kinnison (dkin@ucar.edu).

References

Baldwin, M. P., Gray, L. J., Dunkerton, T. J., Hamilton, K., Haynes, P. H., Randel, W. J., et al. (2001). The quasi-biennial oscillation. *Reviews of Geophysics*, *39*, 179–229. https://doi.org/10.1029/1999RG000073

Ball, W. T., Alsing, J., Mortlock, D. J., Staehelin, J., Haigh, J. D., Peter, T., et al. (2018). Continuous decline in lower stratospheric ozone off sets ozone layer recovery. *Atmospheric Chemistry and Physics*, *18*, 1379–1394. https://doi.org/10.5194/acp-18-1379-2018

Camp, C. D., Roulston, M. S., & Yung, Y. L. (2003). Temporal and spatial patterns of the interannual variability of total ozone in the tropics. *Journal of Geophysical Research*, *108*(D20), 4643. https://doi.org/10.1029/2001JD001504

Camp, C. D., & Tung, K.-K. (2007). The influence of the solar cycle and QBO on the late-winter stratospheric polar vortex. *Journal of the Atmospheric Sciences*, *64*(4), 1267–1283. https://doi.org/10.1175/JAS3883.1

Chipperfield, M. P., Bekki, S., Dhomse, S., Harris, N. R. P., Hassler, B., Hossaini, R., et al. (2017). Detecting recovery of the stratospheric ozone layer. *Nature*, *549*(7671), 211–218. https://doi.org/10.1038/nature23681

Davis, S. M., Rosenlof, K. H., Hassler, B., Hurst, D. F., Read, W. G., Vömel, H., et al. (2016). The Stratospheric Water and Ozone Satellite Homogenized (SWOOSH) database: A long-term database for climate studies. *Earth System Science Data*, *8*(2), 461–490. https://doi.org/10.5194/essd-8-461-2016

Harris, N. R. P., Hassler, B., Tummon, F., Bodeker, G. E., Hubert, D., Petropavlovskikh, I., et al. (2015). Past changes in the vertical distribution of ozone—Part 3: Analysis and interpretation of trends. *Atmospheric Chemistry and Physics*, *15*(17), 9965–9982. https://doi.org/10.5194/acp-15-9965-2015

Jackman, C., Fleming, E., Vitt, F., & Considine, D. (1999). The influence of solar proton events on the ozone layer. *Advances in Space Research*, *24*(5), 625–630. https://doi.org/10.1016/S0273-1177(99)00481-0

Jackman, C. H., Marsh, D. R., Vitt, F. M., Garcia, R. R., Fleming, E. L., Labow, G. J., et al. (2008). Short- and medium-term atmospheric effects of very large solar proton events. *Atmospheric Chemistry and Physics Discussions*, *7*(4), 10,543–10,588. https://doi.org/10.5194/acpd-7-10543-2007

Jackman, C. H., Marsh, D. R., Vitt, F. M., Garcia, R. R., Randall, C. E., Fleming, E. L., & Frith, S. M. (2009). Long-term middle atmospheric influence of very large solar proton events. *Journal of Geophysical Research*, *114*, D11304. https://doi.org/10.1029/2008JD011415

Jonsson, A. I., de Grandpré, J., Fomichev, V. I., McConnell, J. C., & Beagley, S. R. (2004). Doubled CO_2-induced cooling in the middle atmosphere: Photochemical analysis of the ozone radiative feedback. *Journal of Geophysical Research*, *109*, D24103. https://doi.org/10.1029/2004JD005093

Kinnison, D. E., Brasseur, G. P., Walters, S., Garcia, R. R., Marsh, D. R., Sassi, F., et al. (2007). Sensitivity of chemical tracers to meteorological parameters in the MOZART-3 chemical transport model. *Journal of Geophysical Research*, *112*, D20302. https://doi.org/10.1029/2006JD007879

Kuttippurath, J., & Nair, P. J. (2017). The signs of Antarctic ozone hole recovery. *Scientific Reports*, *7*(1), 585. https://doi.org/10.1038/s41598-017-00722-7

Li, F., Stolarski, R. S., & Newman, P. A. (2009). Stratospheric ozone in the post-CFC era. *Atmospheric Chemistry and Physics*, *9*(6), 2207–2213. https://doi.org/10.5194/acp-9-2207-2009

Marsh, D. R., Mills, M. J., Kinnison, D. E., Lamarque, J.-F., Calvo, N., & Polvani, L. M. (2013). Climate change from 1850 to 2005 simulated in CESM1 (WACCM). *Journal of Climate*, *26*(19), 7372–7391. https://doi.org/10.1175/JCLI-D-12-00558.1

Merkel, A. W., Harder, J. W., Marsh, D. R., Smith, A. K., Fontenla, J. M., & Woods, T. N. (2011). The impact of solar spectral irradiance variability on middle atmospheric ozone. *Geophysical Research Letters*, *38*, L13802. https://doi.org/10.1029/2011GL047561

Mills, M. J., Schmidt, A., Easter, R., Solomon, S., Kinnison, D. E., Ghan, S. J., et al. (2016). Global volcanic aerosol properties derived from emissions, 1990–2014, using CESM1 (WACCM). *Journal of Geophysical Research: Atmospheres*, *121*, 2332–2348. https://doi.org/10.1002/2015JD024290

Neely, R. R. I., & Schmidt, A. (2016). VolcanEESM: Global volcanic sulphur dioxide (SO_2) emissions database from 1850 to present—Version 1.0. *Centre for Environmental Data Analysis*. https://doi.org/10.5285/76ebdc0b-0eed-4f70-b89e-55e606bcd568

Newchurch, M. J., Yang, E.-S., Cunnold, D. M., Reinsel, G. C., Zawodny, J. M., & Rusell, J. M. III (2003). Evidence for slowdown in stratospheric ozone loss: First stage of ozone recovery. *Journal of Geophysical Research*, *108*(D16), 4507. https://doi.org/10.1029/2003JD003471

Portmann, R. W., Solomon, S., Garcia, R. R., Thomason, L. W., Poole, L. R., & McCormick, M. P. (1996). Role of aerosol variations in anthropogenic ozone depletion in the polar regions. *Journal of Geophysical Research*, *101*, 22,991–23,006. https://doi.org/10.1029/96JD02608

Reinsel, G. C., Weatherhead, E., Tiao, G. C., Miller, A. J., Nagatani, R. M., Wuebbles, D. J., & Flynn, L. E. (2002). On detection of turnaround and recovery in trend for ozone. *Journal of Geophysical Research*, *107*(D10), 4078. https://doi.org/10.1029/2001JD000500

Seppälä, A., Verronen, P. T., Kyrölä, E., Hassinen, S., Backman, L., Hauchecorne, A., et al. (2004). Solar proton events of October-November 2003: Ozone depletion in the Northern Hemisphere polar winter as seen by GOMOS/Envisat. *Geophysical Research Letters*, *31*, L19107. https://doi.org/10.1029/2004GL021042

Shaw, T. A., & Perlwitz, J. (2014). On the control of the residual circulation and stratospheric temperatures in the Arctic by planetary wave coupling. *Journal of the Atmospheric Sciences*, *71*(1), 195–206. https://doi.org/10.1175/JAS-D-13-0138.1

Solomon, S., & Crutzen, P. J. (1981). Analysis of the August 1972 solar proton event including chlorine chemistry. *Journal of Geophysical Research*, *86*, 1140–1146. https://doi.org/10.1029/JC086iC02p01140

Solomon, S., & Garcia, R. R. (1984). On the distributions of long-lived tracers and chlorine species in the middle atmosphere. *Journal of Geophysical Research*, *89*, 11,633–11,644. https://doi.org/10.1029/JD089iD07p11633

Solomon, S., Garcia, R. R., & Stordal, F. (1985). Transport processes and ozone pertubations. *Journal of Geophysical Research*, *90*, 12,981–12,989. https://doi.org/10.1029/JD090iD07p12981

Solomon, S., Ivy, D., Gupta, M., Bandoro, J., Santer, B., Fu, Q., et al. (2017). Mirrored changes in Antarctic ozone and stratospheric temperature in the late 20th versus early 21st centuries. *Journal of Geophysical Research: Atmospheres*, *122*, 8940–8950. https://doi.org/10.1002/2017JD026719

Solomon, S., Ivy, D. J., Kinnison, D., Mills, M. J., Neely, R. R., & Schmidt, A. (2016). Emergence of healing in the Antarctic ozone layer. *Science*, *310*, 307–310. https://doi.org/10.1126/science.aae0061

Solomon, S., Kinnison, D., Bandoro, J., & Garcia, R. (2015). Simulation of polar ozone depletion: An update. *Journal of Geophysical Research: Atmospheres*, *120*, 7958–7974. https://doi.org/10.1002/2015JD023365

Solomon, S., Portmann, R. W., Garcia, R. R., Randel, W., Wu, F., Nagatani, R., et al. (1998). Ozone depletion at mid-latitudes: Coupling of volcanic aerosols and temperature variability to anthropogenic chlorine. *Geophysical Research Letters*, *25*, 1871–1874. https://doi.org/10.1029/98GL01293

Steinbrecht, W., Claude, H., & Winkler, P. (2004). Enhanced upper stratospheric ozone: Sign of recovery or solar cycle effect? *Journal of Geophysical Research*, *109*, D02308. https://doi.org/10.1029/2003JD004284

Steinbrecht, W., Froidevaux, L., Fuller, R., Wang, R., Anderson, J., Roth, C., et al. (2017). An update on ozone profile trends for the period 2000 to 2016. *Atmospheric Chemistry and Physics*, *17*(17), 10,675–10,690. https://doi.org/10.5194/acp-17-10675-2017

Strahan, S. E., & Douglass, A. R. (2018). Decline in Antarctic Ozone Depletion and Lower Stratospheric Chlorine Determined From Aura Microwave Limb Sounder Observations. *Geophysical Research Letters*, *44*. https://doi.org/10.1002/2017GL074830

Tummon, F., Hassler, B., Harris, N. R. P., Staehelin, J., Steinbrecht, W., Anderson, J., et al. (2015). Intercomparison of vertically resolved merged satellite ozone data sets: Interannual variability and long-term trends. *Atmospheric Chemistry and Physics*, *15*(6), 3021–3043. https://doi.org/10.5194/acp-15-3021-2015

Xie, F., Li, J., Tian, W., Zhang, J., & Sun, C. (2014). The relative impacts of El Niño Modoki, canonical El Niño, and QBO on tropical ozone changes since the 1980s. *Environmental Research Letters*, *9*(6). https://doi.org/10.1088/1748-9326/9/6/064020